Role of small-sized phytoplankton in triggering an ecosystem disruptive algal bloom in a Mediterranean hypersaline coastal lagoon

Jesús M. Mercado[1*], Dolores Cortés[1], Francisco Gómez-Jakobsen[1], Candela García-Gómez[1], Sophia Ouaissa[2], Lidia Yebra[1], Isabel Ferrera[1], Nerea Valcárcel[1], María López[1], Rocío García Muñoz[3], Aranzazu Ramos[3], Jaime Bernardeau[3], María Dolores Belando[3], Eugenio Fraile-Nuez[4], Juan M. Ruíz[3]

[1]Centro Ocenográfico de Málaga. Instituto Español de Oceanografía. Puerto Pesquero s/n. 29640, Fuengirola (Málaga). Spain

[2]Programa de Doctorado Diversidad Biológica y Medioambiente. Facultad de Ciencias, Universidad de Málaga. Campus de Teatinos, 29071, Málaga. Spain

[3]Centro Oceanográfico de Murcia. Instituto Español de Oceanografía. Varadero 1. Apdo. 22. 30740, San Pedro del Pinatar (Murcia). Spain

[4]Centro Oceanográfico de Canarias. Instituto Español de Oceanografía. C/ Farola del Mar, 22, 38180, Santa Cruz de Tenerife. Spain

*Corresponding author: jesus.mercado@ieo.es

Abstract

Monthly samplings carried out in 2016-2019 and satellite color images of 2002-2019 have been combined to determine the onset and causative species of the ecosystem disruptive algal bloom (EDAB) that affects the Mar Menor coastal lagoon since 2015. Substantial changes in satellite spectral reflectance attributable to increasing abundance of *Synechococcus* were registered in 2014. Furthermore, cell abundances of this species in 2016 were the largest ever obtained in the lagoon (6 10^6 cells mL^{-1}), with values similar to those reported for other Mediterranean hypertrophic estuaries and coastal lagoons. These results suggest that the early changes leading to the EDAB started in 2014 and that *Synechococcus* played a relevant role in its development. Diatom and dinoflagellate abundances changed substantially in 2016-2019, ranging from 10^2 to more than 10^4 cells mL^{-1}. Some of these changes were linked to flood, suggesting that EDAB has modified substantially the homestatic capacity of the lagoon.

Keyword: Algal bloom, Diatoms, Dinoflagelattes, eutrophication, nutrients, *Synechococcus*

Highlights

Synechococcus had a key role in the onset of the ecosystem disruptive algal bloom

Eutrophication has produced a significant alteration of the lagoon phytoplankton

Self-regulation of the Mar Menor in response to environmental changes has reduced

1. Introduction

Coastal lagoons are among the most threatened marine ecosystems since human pressures in the catchment areas often releases nutrients that may lead to eutrophication (Cloern, 2001), whose effects are amplified by global climate change (Lloret et al., 2008). Numerous studies link eutrophication events in coastal areas with the increasing incidence of long-term harmful algal blooms that disrupt or degrade the structure and function of the ecosystem (the so called 'ecosystem disruptive algal blooms', EDABs; Lomas et al., 2004; Sunda et al., 2006). In coastal lagoons, where macrophyte communities play a key role in maintaining the ecological balance (McGlathery et al., 2007), EDABs produce benthic-pelagic mismatches that contribute to the collapse of the ecosystem (Glibert et al., 2010; Fertig et al., 2013). The species known to cause EDABs belong to fairly dissimilar taxon, including cyanobacteria (*Synechoccocus* and *Nodularia spumigena*), pelagophytes (*Aureoumbra lagunensis* and *Aureococcus anophagefferens*), trebouxiophyte (*Nannochloris atomus*), eustigmatophyte (*Nannochloropsis*), haptophytes (*Chrysochromulina polylepis* and *Prymnesium parvum*) and dinoflagellates (Liu and Buskey, 2000; Trice et al., 2004; Sunda et al., 2006; Michaloudi et al., 2008; Sunda and Shertzer, 2012; Majaneva et al., 2012; Zhang et al., 2015). According to Sunda et al. (2006), all these species producing EDABs share as a common feature their small size and, possibly, their ability for using organic nutrient forms, given that their capacity for assimilating inorganic nutrients is not higher than in other species causing blooms. Some reports also suggest that their toxicity or low palatability for herbivore predators may contribute to the disruption of the trophic dynamics (Sunda et al., 2012). Consequently, not only the available nutrients but also

75 the trophic interactions maybe key factors in determining the triggering of the EDABs.
76 In turn, the diversity of species causing EDABs could imply that the specific
77 environmental factors triggering the bloom differ from one to another coastal system.
78 The EDABs species identification is therefore essential to understand the origin of a
79 disruptive event and, ultimately, to implement effective management strategies (Cloern,
80 2001).

81 One of the most recent EDABs reported in the Mediterranean Sea has occurred
82 in the Mar Menor, the largest hypersaline lagoon in the Western Mediterranean Sea,
83 where strong deterioration of the water quality and benthic communities was
84 appreciated for the first time in 2016 (Belando et al., 2019a; Erena et al., 2019; Pérez-
85 Ruzafa et al., 2019). Previously, the Mar Menor lagoon was classified as an oligotrophic
86 system with chlorophyll concentrations in the water column being normally below 1 μg
87 L^{-1} (Más-Hernández, 1996; Gilabert, 2001; Perez-Ruzafa et al., 2005; Lloret et al.,
88 2008). Extensive presence of benthic macrophyte communities that in fact covered
89 almost 100% of the bottom was another singular feature of the lagoon (Terrados and
90 Ros, 1991; Belando et al., 2019b). The reduction of the water quality detected at the end
91 of 2015 was accompanied by a drastic decrease in water transparency and an increase in
92 chlorophyll concentration above 15 μg L^{-1} en 2016 (Belando et al., 2019a; Erena et al.,
93 2019; García-Oliva, 2019; López-Ballesteros, 2019). Since then, a strong deterioration
94 of the macrophyte communities has occurred, leading to a reduction of 85.8% in 2016
95 (Belando et al., 2019b). Although the first symptoms of this episode were detected in
96 2015, samplings aimed at describing the causes did not start until the second quarter of
97 2016, when the deterioration of the quality of water was already critical. Consequently,
98 the exact onset of the EDAB as well as the causative species during the initial phase
99 have not been determined. Some data published on the phytoplankton composition from

May to December of 2017 indicate that the abundances of *Synechococcus*, Chlorophyceae, Chrysophycea and nanoplanktonic Cryptophycea were higher during that period compared with previously collected data (Soria et al., 2019). These results, together with certain observations in samples collected in 2016 (Ruíz et al., 2016) show abnormal high abundance of small cells which led to the yet unproven hypothesis that the phytoplankton community was dominated by picoplanktonic organisms during the first stages of the bloom.

The objective of this work is to analyze the dynamics of the phytoplankton community during the early development phases of the ecosystem disruptive event in the Mar Menor lagoon in order to: (1) estimate the onset of the bloom, (2) identify the possible causative species and (3) characterize the subsequent shifts in the community. To complete these goals, satellite color images from 2002 to 2019 were gathered and analyzed in combination with environmental and phytoplankton composition data collected in the Mar Menor lagoon from May 2016 to October 2019.

2. Materials and Methods

2.1. Satellite and meteorological data

Ocean color images obtained from the platform MODIS-Aqua were used to retrieve spectral reflectance. The satellite provides a daily image of the study area with a spatial resolution of 1.1 km × 1.1 km. All the Level 2 scenes covering the central part of the lagoon from August 2002 to October 2019 were downloaded from the NASA website (https://oceancolor.gsfc.nasa.gov/reprocessing/r2018/aqua/). Those scenes inadequate for the analysis due to sun glitter and/or the presence of clouds or fog were

discarded, and only valid scenes were used. The MODIS sensor provides reflectance values at 412, 443, 469, 488, 531, 547, 555, 645, 667 and 678 nm. The reflectance for each scene was normalized by blue reflectance at 412 or 443 nm (R_n). For our analyes, the reflectance values from the nearest pixel to the center lagoon (Fig. 1; Longitude:-0.789ºW and Latitude: 37.735ºN) was used to build time series of R_n. This point was located in the lagoon area with maximal depth; therefore, our reflectance time series was not influenced by bottom reflectance as in fact it was assessed by Erena et al. (2019) in their analysis of the satellite images of the Mar Menor in 2017.

Daily data of air temperature near the surface and rainfall from 2002 to 2019 were gathered from the meteorological station of the Spanish Meteorological Agency located just in the shore of the lagoon at San Javier town (http://www.aemet.es; Fig. 1). Atmospheric temperature anomalies were calculated by subtracting the temperature seasonal cycle from the raw time series.

2.2. Samplings and analyses of nutrients, chlorophyll and phytoplankton absorption

Monthly samplings of nutrients and phytoplankton communities were performed in three distinct stations of the lagoon (Fig. 1) from May 2016 to October 2019 (note that samplings could not be performed during some monthly periods). At each point, samples were collected by triplicate with Niskin bottles at 3-4 m depth. Previous samplings indicated the absence of any kind of water column stratification so that samples collected at that intermediate depth can be considered representative of the whole water column. Data of salinity and temperature were taken with a Multiparametric portable meter probe MultiLine ® Multi 3620 (WTW-Xylem

149 Analytics, Germany). PAR irradiance profiles were measured each meter from the sub-
150 surface to the bottom with a LI-1500 data logger (LI-COR, Germany).
151 In the laboratory, water aliquots were either preserved or immediately analyzed
152 depending on the target variable. For nutrient analyses, two replicates of water were
153 immediately frozen at -20ºC. Afterwards, nutrients (nitrate plus nitrite, nitrite,
154 phosphate and silicate) were analyzed by means of segmented flow analysis using a
155 Bran-Luebbe AA3 autoanalyzer, following the methods described in Ramírez et al.
156 (2005). The detection limits were: 0.05 μM for nitrate, 0.01 μM for nitrite, 0.04 μM for
157 phosphate and 0.10 μM for silicate. A total of 0.5 L of water were filtered through
158 Whatman GF/F filters for determination of chlorophyll *a* concentration (Chl *a*) by
159 spectrophotometry after overnight extraction in 90% acetone at 4-5 ºC (SCOR-
160 UNESCO 1966). Two-three mL samples were fixed with glutaraldehyde (1% f.c.) and
161 immediately frozen at -80ºC for the counting of picoplankton by means of flow
162 cytometry (Vaulot et al. 1989). Additionally, 250 mL of water sample were fixed in
163 dark glass bottles with Lugol's solution (2% f.c.) for microscopy taxonomic
164 identification analyses.
165 In addition to the monthly samplings, four intensive surveys were performed in
166 November 2016 and February-, June- and September 2017. During these samplings,
167 samples of chlorophyll were collected at 42 stations covering the whole surface of the
168 lagoon at two or three depths depending on the station. These samples were used to
169 obtain light absorption spectra of non-living matter and phytoplankton.
170 Data of chlorophyll obtained in 2002-2005 from the project EUROGEL (Fuentes
171 et al., 2011) have been also gathered and used for making comparisons with the results
172 obtained from the monthly samplings described above. In the framework of the project
173 EUROGEL, the Spanish Institute of Oceanography performed monthly samplings at 36

stations distributed by the whole Mar Menor. Methods of sampling and analysis of chlorophyll used in that project were similar to the ones previously described.

2.3. Analysis of phytoplankton composition and optical properties

Autotrophic picoplankton were analyzed on a Becton Dickinson FACScan flow cytometer. Counting of cells was performed based on the forward-light scatter (FLS) and the orange and red fluorescence signals. This analysis allowed the identification of *Synechococcus* and eukaryotic picoplankton as the main components of the community. Additionally, Mamiellophyceae were discriminated from other eukaryotic picoplankton according to the FLS signal. Absolute counts were calculated by estimating the flow rates using TruCount™ bead suspensions prepared by adding deionised water to TruCount™ tubes (Becton Dickinson, Franklin Lakes, USA). Abundance of diatoms and dinoflagellates were determined following the technique developed by Utermöhl (1958) by settling 50 or 25 mL of each fixed sample in a composite chamber for 24 h. Cells were counted at 200x and 600x with a Nikon Eclipse TS100 inverted microscope. The species nomenclature was validated following Tomas (1997). Note that samples collected after January 2019 were not analyzed by microscope.

Non-living matter and phytoplankton light absorption was estimated with the filter concentration technique by using the procedure described in Mercado et al. (2008). Half liter of seawater was filtered through a glass fiber filter Wathman GF/F and immediately frozen at -20ºC until further analysis in the lab. Absorbance spectra of the particulate matter (OD_{NAP+AP}) were obtained by placing the filters in the optical path of the spectrophotometer (Cary UV-VIS) and measuring the absorbance each nm from 400 to 750 nm against reference of a glass filter wetted with filtered seawater. Later, in order to determine the absorption spectra of the non-living matter, the filters were dipped in

90% acetone and sonicated during five minutes to improve pigment extraction. Pigments were extracted overnight at 4 ºC. Afterwards, the filters were air exposed until acetone was evaporated and then were wetted in filtered seawater. Absorbance of the filters after extraction (OD_{NAP}) was measured as mentioned above. A glass fiber filter subjected to the same process was used in the reference cell.

Spectral absorbances of the filters before and after extraction was corrected by absorbance at 750 nm, transformed in absorbance of the suspension (OD_{susp}) using the equation proposed by Cleveland and Weidemann (1993) and then used to calculate absorption coefficients of particulate (a_{NAP+AP}) and non-living (a_{NAP}) matter with the formula:

$$a(\lambda) = 2.3\ OD_{susp}(\lambda) / (V/A)$$

where V is the filtered volume (m^3) and A is the filtered area (m^2).

Absorption coefficient of the phytoplankton [$a_{AP}(\lambda)$ (m^{-1})], was calculated by subtracting $a_{NAP}(\lambda)$ to $a_{NAP+AP}(\lambda)$. Chlorophyll *a* specific absorption spectra [$a^*(\lambda)$ (m^2 mg Chla^{-1}], were calculated by dividing $a_{AP}(\lambda)$ to Chl *a* estimated from the pigment extracts as described above.

2.4. Statistical analyses

The daily data of satellite reflectance were used to generate monthly time series that were analyzed with the functions *st* and *decompose* of R (R core Team 2013). As a result, the monthly time series were split out into seasonal, trend and irregular components. A principal component analysis was performed with the trend series of R_n

by using the function *rda* with the R-package *vegan* (Oksanen et al., 2013). In order to investigate the main variables influencing the phytoplankton community composition, a canonical correspondence analysis (CCA) was performed by using the pool of environmental variables (temperature, salinity, chlorophyll and nutrient concentrations) as constraining variable and the abundances of the different phytoplankton groups (diatoms, dinoflagellates, *Synechococcus*, Mamiellophyceae and other picoeukaryotes) as the constrained variables. R_n of some selected spectral bands were also included into the pool of constraining variables to determine possible associations between the communities and the reflectance signal captured by the satellite. Only the monthly sampling periods for which all the variables were analyzed were used for this analysis. CCA was also carried out with the function *cca* of the *vegan* R-package.

3. Results

The analysis of the time series of averaged monthly satellite reflectance at wavelengths representative of the main colour bands (R_n488, R_n555 and R_n645) from 2002 to 2019 reveals that the reflectance features of the Mar Menor changed substantially since the last quarter of 2013. Note that these changes were not preceded by remarkable temperature atmospheric anomalies. Since that date, the monthly means of $R_{rs}645$ started to increase steeply (Fig. 2) reaching a maximal peak in March 2016. Additionally, high values of R_n488 and R_n555 were obtained in 2014. R_n488, R_n555 and R_n645 decreased substantially since March 2016 until reaching minimum values in 2018. These temporal change patterns in R_n were assessed with a principal component analysis (Fig. 3). The scores of each reflectance band for PC1 (which explained 69% of the variance) were positive indicating that this variance component discriminated

monthly means according to the intensity of R_n irrespectively of the spectral band (although the scores of PC1 were comparatively higher for R_n547 and R_n555). The reflectance red bands had positive scores for PC2 (that explained 29% of variance) while reflectance of the blue bands had negative scores. In contrast, the green bands did not contribute to PC2. The scores of PC1 and PC2 for each monthly period (Fig. 3b) show clearly that PC2 discriminated the observations beginning with April 2014 from the rest of the time series. For that period, PC2 positive scores (i.e. higher contribution of the reflectance red bands) were obtained, with maximal contributions from March 2015 to June 2016. Note that PC1 scores decreased progressively after that period.

Monthly means of Chl *a* calculated with data of the three stations sampled from May 2016 to October 2019 are shown in Fig. 4 along the daily data of R_n488, R_n555 and R_n645. Chl *a* ranged from less than 1 to 12 $\mu g\ L^{-1}$ for the whole sampling period. The available data for 2003-2004 were close to this lower limit (Fig. 4b). Higher Chl *a* roughly matched with pronounced monthly peaks of R_n645 and R_n667 in 2016-2019. In fact, for that time period, there was a significant correlation between R_n555/R_n645 ratio and Chl *a* (both in logarithmic scales; Fig. 4b), indicating that R_n increasing in the red reflectance bands paralleled the increases in Chl *a* observed during the different phases of the EDAB. This correlation was not significant in 2003-2004; therefore, the dependence of R_n555/R_n645 ratio on Chl *a* appears to occur exclusively during the EDAB.

As shown in Table 1, the analyzed environmental factors also presented large variation ranges in 2016-2019. Water temperature ranged more than 20 ºC, with a minimum in January 2017 coinciding with a flood episode that produced a substantial runoff water discharge from the catchment towards the lagoon and a consequent drastic reduction in salinity. Associated to this heavy rainfall event, high nitrate and low silicate

concentrations were obtained at the beginning of 2017. In contrast, higher phosphate concentrations were obtained in 2018 when silicate also decreased steeply. Note that in that annual period, significant heavily rainfall episodes were absent and salinity remained above 43.0 during all year. Therefore, these changes in nutrient concentrations occurred in 2018 apparently cannot be attributed to significant variations in runoff water discharges.

The abundances of the main phytoplankton groups identified in the monthly samplings are shown in Fig. 5 (note that there are not data for diatoms or dinoflagellates quantified by microscope after January 2019). Overall, *Nitzschia*, *Cyclotella*, *Cylindrotheca* and *Chaetoceros* were the most abundant genera. The highest abundance of diatoms was obtained at the beginning of 2017 when more than 12,500 cell mL^{-1} were found due to a bloom of *Nitzschia* sp. Since that date, diatom abundance decreased steeply with a minimum in mid-2017. Afterwards, in 2018, some diatom abundance peaks attributable to *Cyclotella* sp. were produced although they were lower than the one occurred in 2017. Dinoflagellates were about one magnitude order less abundant than diatoms and abundances of the two groups were uncorrelated ($n=24$; $r^2=0.08$; $p>0.05$). The highest abundance of dinoflagellates was obtained in summer 2016 when the community was dominated by *Prorocentrum*. Dominance of this genus over other dinoflagellates also occurred in different monthly periods of 2017 and 2018. In September 2016 we found that *Gymnodinium* was more abundant than *Prorocentrum* as well as un-classified cells at genus level did in several monthly periods, particularly in 2018.

Abundance of *Synechoccocus* ranged by two magnitude orders (Fig. 6), with maxima up 6 10^6 cell mL^{-1} in August 2016, November 2017 and January 2018. Mamiellophyceae also reached abundance peaks up to 4.5 10^6 cell mL^{-1} in 2016-2017

297 although this picoeukaryotic group was only present in sufficient abundance for
298 quantification in summer or early fall. The other picoeukaryotes had a variability range
299 comparatively low (from 2.9 10^3 to 7.0 10^4 cell mL^{-1}) and were less abundant than
300 *Synechococcus* in all analyzed samples.

301 The factors influencing the phytoplankton composition were assessed with a
302 canonical correspondence analysis (CCA, Fig. 6). The two first variance components of
303 the CCA explained 52% and 28% of variability, respectively. Diatoms and
304 Mamiellophyceae had the highest scores for CCA1, although with opposite signs. All
305 samples with positive score for CCA1 presented abundances of diatoms higher than 5.9
306 10^2 cell mL^{-1} and the samples with presence of Mamiellophyceae had negative scores.
307 Therefore, CCA1 discriminated the samples mainly according to the relative
308 contribution of both phytoplankton groups. *Synechococcus* presented the highest score
309 for CCA2 followed by Mamiellophyceae also with opposite signs; the scores of the
310 other phytoplankton groups for this variance component were notably low. Therefore,
311 CCA2 discriminated samples according to their *Synechococcus* abundance relative to
312 the other phytoplankton groups. The main environmental variables constraining the
313 phytoplankton community composition were salinity, temperature and nitrate and
314 silicate concentrations; the CCA1 scores for nitrate were positive while for silicate and
315 salinity were negative indicating that, overall, the importance of diatoms was higher
316 when nitrate concentrations increased. In turn, *Synechococcus* was strongly associated
317 with temperature and salinity. It is interesting to note that CCA1 scores of R_n469, R_n531
318 and R_n555 were fairly low (R_n645 and R_n667 had scores only a little higher) indicating
319 that variability in diatom abundance was barely reflected in the satellite reflectance
320 spectra of the Mar Menor. In contrast, all the reflectance bands (apart from R_n555)
321 presented high scores for CCA2 compared to the other variables. Particularly, the CCA

biplot indicates that *Synechococcus* was strongly associated to R_n645 and R_n667 suggesting that changes in the relative abundance of this phytoplankton group affected the signal captured by the satellite in these reflectance bands.

In order to assess how the changes in abundance and composition of phytoplankton affected the optical properties of the water column, light absorption spectra of the particulate matter obtained in the four intensive samplings performed in 2016-2017 were analyzed (Fig. 8). For the four samplings, the mean spectra show absorption coefficient peaks in the blue bands at 440, 460 and 495 nm which are attributable to carotenoids absorption. These peaks were more pronounced in November 2016 and October 17 and less in February 2017 and June 2017 (particularly the absorption peak at 495 nm). Additionally, there were absorption peaks at 545- and 620 nm coinciding with the absorption maxima of cyanobacteria attributable to phycobilins. Note that the absorption percentage by particulate material attributable to non-algal particles (i.e. after pigment extraction) presented minima in the absorption red bands around these peaks (Suppl. Fig. 1), indicating that phytoplankton was the main optical component that contributed to these absorption peaks.

4. Discussion

The anthropogenic pressures on the Mar Menor have increased during the last decades due to population growth and spread of the irrigated agricultural surface area that in fact duplicated from 1988 to 2008 (Carreño, 2015). Leachate from the irrigated area has produced increasing loads of dissolved nitrogen in the ground water that drains into the lagoon; particularly, nitrate has experienced a notable increase with concentrations in ground water of about 22-45 mg L^{-1} (Ruíz et al., 2020). Heavy rain

episodes that feature the Mediterranean weather have also contributed to carry these nutrients from the drainage basin towards the lagoon. It can be concluded that the lagoon has suffered an eutrophication pressure since the 1980s-1990s that would be aggravated by its low water renewal rate (around 360 days; García-Oliva et al., 2019; Ruíz et al., 2020). However, as far as we know, visible symptoms of eutrophication such as phytoplankton blooms, reduction in water transparency or decline of the macrophyte communities had not been noticed before 2015 (Erena et al., 2019; Pérez-Ruzafa et al., 2019) and the start date of the lagoon ecosystem deterioration has not been determined.

Our data indicate that the satellite spectral reflectance of the Mar Menor changed substantially since 2013 compared to previous periods of the analyzed dataset (2002-2013). Different phytoplankton species have unique light absorption and backscattering properties determined by their shape, cell structure and pigment composition, which influence their reflectance spectra. Therefore, the observed changes in 2014 could be an indicator of the phytoplankton shifts which, in turn, dealt to the EDAB. Satellite reflectance has been used to remotely identify causative species of blooms (Warner and Fan, 2013; Simis et al., 2005). Particularly, phytoplankton communities dominated by cyanobacteria have been identified from the unique absorption peaks of phycobilins around 530-550 nm and 620 nm (Roy et al., 1989) that produce minimum of R_n at 620 nm followed by local maximum at 650 nm (Simis et al., 2005; Wojtasiewizc and Ston-Egiert, 2016). In the Mar Menor, the main change in the satellite reflectance consisted of increases in R_n645 that could therefore be attributed to the optical signature of cyanobacteria. Concordantly, the results of the CCA clearly indicate that the abundances of *Synechococcus* in 2016-2018 was tightly related to variability in the blue R_n bands. Furthermore, the absorption spectra obtained from the intensive samplings in

2016-2017 show absorption peaks at 620 nm that can be attributable to cyanobacteria. Note that the non-living matter absorption spectra presented a local minimum at this wavelength which reinforces the hypothesis that any increase in R_n645 might be attributable to phytoplankton. It has to be noted that diatoms could also contribute to increase in reflectance of the blue band due to absorption by chlorophyll c1 and c2; however, the high abundances of diatoms obtained during some monthly sampling periods were not reflected in our R_n values, as demonstrated from the CCA results. Consequently, our data support that the increasing presence of *Synechococcus* featured the start of the EDAB.

The data of abundance and composition of the phytoplankton communities also indicate that the abundance values of *Synechococcus* obtained in our analyses for 2016 (and afterwards) are higher than the those ones published previously. Ghai et al. (2012) analyzed the composition of the picoplankton communities in the Mar Menor in 2010 and showed that *Synechococcus* was the only free-living cyanobacteria identified in the lagoon by genetic methods as well as the phytoplankton community was dominated by dinoflagellates. The abundance of *Synechococcus* reported in that article (estimated by inverted microscopy) is about one order of magnitude lower than the abundance maxima obtained in our analysis (i.e. $5\ 10^6$ cells mL^{-1}). Furthermore, the maximal abundances obtained in our study are comparable with those described for another Mediterranean coastal lagoon nearby the Mar Menor, the Albufera in Valencia, which has been classified as hypertrophic and whose phytoplankton community is dominated by cyanobacteria (Romo et al., 2008). Our maximal abundances of *Synechococcus* are also close to those observed in other Mediterranean hypertrophic estuaries and coastal lagoons (Caroppo, 2000; Camacho et al., 2003). Based on these results, we conclude that *Synechoccocus* had a relevant role in the onset of the EDAB occurred in the Mar

Menor as has been reported for other lagoons affected by this process (Phlips et al., 1999; Glibert et al., 2004).

Irrespectively of the nutrient enrichment suffered by the lagoon during the last decades (which created the necessary environment for stimulating algal growth), the specific factor that triggered the EDAB in the Mar Menor is still unknown. Our data indicate that significant positive anomalies of atmospheric temperature occurred in 2014-2016 when, in contrast, negative anomalies were reduced, indicating that this period was abnormally warm. Our results show that increasing abundance of *Synechococcus* was linked to increase of temperature in 2016-2019. Therefore, this factor would have contributed to the development of the EDABs. Nevertheless, the *Synechococcus* bloom is not necessarily a direct consequence of temperature increasing as this pressure should affect the whole ecosystem. Sunda et al. (2006) and Sunda and Shertzer (2012) have shown that the trophic interactions play an determinant role in the dynamics of the EDABs. According to these authors, competition of phytoplankton species by different nutrient sources (including organic forms) and differential grazing on these species are key factors in development of EDABs. In that sense, Pérez-Ruzafa et al. (2019) pointed out that grazing exerted on phytoplankton by herbivores explains the low levels of Chl *a* in the lagoon before the EDAB, suggesting that loss of predators could have been a key factor in that process. Yet, data supporting this hypothesis have not been presented so far. However, it could be speculated that the predator absence would be a consequence (better than a cause) of the *Synechococcus* bloom. Our data indicate that the initial bloom occurred along with notably changes in the phytoplankton composition possibly modifying the quality and palatability of the herbivore diet.

The previous data of phytoplankton composition in the Mar Menor are scarce but support that the community in 2016-2019 was fairly different compared to previous

periods. Gilabert et al. (2001) described abundance up 10^3 cells mL^{-1} of *Nitzschia closterium* in summer as well as dominance of *Rhodomonas*, Cryptomonas and *Cyclotella* during the rest of the annual cycle. *Nitzschia* was the most abundant diatom in our study from August 2016 to April 2017 and occasionally afterwards; but its abundance peaks were higher by one magnitude order and did not exhibited any seasonal pattern. Furthermore, substantial interannual changes in the patterns of dominance of diatoms and dinoflagellates were produced in 2016-2018. These data indicate that the alteration in the phytoplankton community persisted afterwards the first phase of the EDAB even although abundance of *Synechococcus* decreased. In our study, diatom abundance was related to time periods with higher nitrate concentrations. These results indicate that the mechanisms regulating the phytoplankton community in the Mar Menor, including both nutrient availability and grazing pressure, have been altered substantially in 2016-2019. As example of this, we reported a substantial reduction of Chl*a* and increasing water clearance in 2018, with values similar to those one observed before the EDAB. This change was interpreted as a recovery of the lagoon ecosystem was occurring (Pérez-Ruzafa et al. 2019). However, Chl *a* increased gradually between March and August 2019 and suddenly in September 2019, when concentrations even higher than those ones found in 2016 were registered. This latter abrupt increase was linked to a flood occurred in that date. These rapid changes in chlorophyll concentration have not been observed in the lagoon before the EDAB supporting that the homestatic capacity of the lagoon has been affected substantially.

Acknowledgements

The samplings and analyses were supported by the projects MEMM (financed by the Spanish Institute of Oceanography), 2-3 ESMAREU (financed by Spanish Ministry of Agriculture, Food and Environment), 10-ESMARES2-C4A2 (financed by Spanish Ministry of Ecological Transition and Demographic Challenge) and UMBRAL (CTM2017-86695-C3-2-R; financed by the National Plan of Research of the Spanish Government). M.D.B., J.B.E. and N.V.P. were supported by a contract within the Program *Personal Técnico de Apoyo* funded by the Ministerio de Economía y Competitividad. We acknowledge logistical support provided by President and Staff of the harbours Club Nautico Lo Pagán, Club Náutico La Puntica and Centro de Actividades Náuticas (San Pedro del Pinatar, Murcia, Spain). We thank Regional Government of Murcia, and national authorities (MITECO) for permission. We thank Project EUROGEL (Grant Agreement ID: EVK3-CT-2002-00074) and Spanish Meteorological Agency (AEMET) for providing data.

Credit Author Statement

Mercado JM: Conceptualization, writing, original draft, sample analysis, data collection; **Cortés D**: sample analysis; **Gómez-Jakobsen F**: data acquisition, formal analysis; **García-Gómez C**: sample collection and analysis; **Ouaissa S**: sample analysis; **Yebra L**: conceptualization, review and editing; **Ferrera I.**: conceptualization, review and editing; **Valcárcel N**: sample collection; **López M**: sample analysis; **García-Muñoz R**: planning of samplings, sample collection and analysis; Aranzazu Ramos: sample collection and analysis; **Bernardeau J**: sample collection and analysis; **Belando MD**: sample collection and analysis; **Fraile-Nuez E**: conceptualization; planning of samplings, review and editing; **Ruíz JM**: conceptualization, management and coordination responsibility for the research activity and execution; sample collection.

References

Belando MD, Bernardeau-Esteller J, Paradinas I, Ramos-Segura A, Garcia-Muñoz R, Garcia-Moreno P, Marin-Guirao L and Ruiz JM (2019a). Assessment of long-term interaction between an opportunistic macroalga and a native seagrass in a Mediterranean coastal lagoon. Front. Mar. Sci. Conference Abstract: XX Iberian Symposium on Marine Biology Studies (SIEBM XX) . doi: 10.3389/conf.fmars.2019.08.00190

Belando, M.D., Ruiz, J.M., Muñoz, R.G., Segura, A.R., Esteller, J.B., Casero, J.J., Guirao, L.M., Moreno, P.G., Navarro, I.F., Nuez, E.F., Mercado, J.M., 2019b. Collapse of macrophytic communities in a eutrophicated coastal lagoon. Front. Mar. Sci. Conference Abstract: XX Iberian Symposium on Marine Biology Studies (SIEBM XX) . doi: 10.3389/conf.fmars.2019.08.00192.

Camacho, A., Picazo, A., Miracle, M.A., Vicente, E., 2003. Spatial distribution and temporal dynamics of picocyanobacteria in a meromictic karstic lake. Archiv für Hydrobiologie 148: 171-184.

Caroppo, C., 2000. The contribution of picophytoplankton to community structure in a Mediterranean brackish environment. J. Plankton Res. 22, 381-397

Carreño, M.F., 2015. Seguimiento de los Cambios de usos y su influencia en las comunidades y hábitats naturales en la cuenca del Mar Menor, 1988-2009, con el uso de SIG y teledetección. Tesis Doctoral. Universidad de Murcia.

Cleveland, J. S., Weidemann, A. D., 1993. Quantifying absorption by aquatic particles: a multiple scattering correction for glass-fiber filters. Limnol. Oceanogr. 38, 1321-1327.

Cloern, J.E., 2001. Our evolving conceptual model of the coastal eutrophication problem. Mar. Ecol. Prog. Ser. 210, 223-253.

Erena, M., Domínguez, J.A., Aguado-Jiménez, F., Soria, J., García-Galiano, S., 2019. Monitoring Coastal Lagoon Water Quality through Remote Sensing: The Mar Menor as a Case Study. Water 11, 11-1468.

Fertig, B., O'Neil, J.M., Beckert, K.A., Cain, C.J., Needham, D.M., Carruthers, T.J.B., Dennison, W.C., 2013. Elucidating terrestrial nutrient sources to a coastal lagoon, Chincoteague Bay, Maryland USA. Estuar. Coast. Shelf Sci. 116, 1–10.

Fuentes, V., Straehler-Pohl, I., Atienza, D., Franco, I., Tilves, U., Gentile, M., Acevedo, M., Olariaga, A., Gili, J.M., 2011. Life cycle of the jellyfish *Rhizostoma pulmo* (Scyphozoa: Rhizostomeae) and its distribution, seasonality and inter-annual

515 variability along the Catalan coast and the Mar Menor (Spain, NW Mediterranean).
516 Mar. Biol. 158,2247–2266.
517 C., Umgiesser, G., McKiver, W., Ghezzo, M., De Pascalis, F., Pérez-Ruzafa, A., 2019.
518 Modelling the impact of dredging inlets on the salinity and temperature regimes in
519 coastal lagoons. Ocean Coast. Manag. 180, 104913.
520 Ghai, R., Hernández, C.M., Picazo, A., Mizuno, C.M., Ininbergs, K., Díez, B., Valas,
521 R., DuPont, C.L., McMahon, K.D., Camacho, A., Rodriguez-Valera, F., 2012.
522 Metagenomes of Mediterranean coastal lagoons. Sci. Reports PMID, 22778901.
523 Gilabert, J., 2001. Seasonal plankton dynamics in a Mediterranean hypersaline coastal
524 lagoon: the Mar Menor. J. Plankton Res. 23, 207–218.
525 Glibert, P.M, Heil, C.A., Hollander, D., Revilla, M., Hoare, A., Alexander, J., Murasko,
526 S., 2004. Evidence for dissolved organic nitrogen and phosphorus uptake during a
527 cyanobacterial bloom in Florida Bay. Mar. Ecol. Prog. Ser. 280, 73-83.
528 Glibert, P.M., J. Boyer, C. Heil, C. Madden, B. Sturgis, and C. Wazniak. 2010. Blooms
529 in Lagoons: different from those of river-dominated estuaries. In Kennish, M., Paerl,
530 H. (eds), Coastal lagoons: critical habitats of environmental change. Boca Raton,
531 Taylor and Francis. 91–114.
532 Hernández, J.M., 1996. El Mar Menor. Relaciones, diferencias y afinidades entre la
533 laguna costera y el mar Mediterráneo adyacente. Ph.D. Thesis. Universidad
534 Autónoma de Madrid, España.
535 Liu, H., Buskey, E.J., 2000. Hypersalinity enhances the production of extracellular
536 polymeric substance (eps) in the texas brown tide alga, *Aureoumbra*
537 *lagunensis* (Pelagopnyceae). J. Phycol. 36, 71-77.
538 Lloret, J., Marín, A.L., 2008. Is coastal lagoon eutrophication likely to be aggravated by
539 global climate change? Est. Coast. Shelf Sci. 78, 403-412.
540 Lomas, M.W., Kana, T.M., MacIntyre, H.L., Cornwell, J.C., Nuzzi, R., Waters, R.,
541 2004. Interannual variability of *Aureococcus anophagefferens* in Quantuck Bay,
542 Long Island: natural test of the DON hypothesis. Harmful Algae. 3, 389–402.
543 López-Ballesteros, A. ,Senent-Aparicio, J., Srinivasan, R., Pérez-Sánchez, J., 2019.
544 Assessing the Impact of Best Management Practices in a Highly Anthropogenic and
545 Ungauged Watershed Using the SW Model: A Case Study in the El Beal Watershed
546 (Southeast Spain). Agronomy 9, 576.

547 Más-Hernández, J.M., 1996. El Mar Menor. Relaciones, diferencias y afinidades entre
548 la laguna costera y el mar mediterraneo adyacente. Ph.D. Thesis. Universidad
549 Autónoma de Madrid, España.
550 McGlathery, K.J., Sundbäck, K., Anderson, I.C., 2007. Eutrophication in shallow
551 coastal bays and lagoons: The role of plants in the coastal filter. Mar. Ecol. Prog. Ser.
552 348, 1-18.
553 Majaneva, M., Rintala, J.M.,Hajdu, S., Hällfors, S., Hällfors, G., Skjevik, A.T.,
554 Gromisz, S., Kownacka, J., Busch, S., Blomster J., 2012. The extensive bloom of
555 alternate-stage *Prymnesium polylepis* (Haptophyta) in the Baltic Sea during autumn–
556 spring 2007–2008. Eur. J. Phycol. 47, 310-320.
557 Mercado, J.M., Ramírez, T., Cortés, D., 2008. Changes in nutrient concentration
558 induced by hydrological variability and its effect on light absorption by
559 phytoplankton in the Alborán Sea (Western Mediterranean Sea). J. Mar. Syst. 71, 31-
560 45.
561 Michaloudi, E., Moustaka-Gouni, M., Gkelis, S., Pantelidakis, K. 2008. Plankton
562 community structure during an Ecosystem Disruptive Algal Bloom of *Prymnesium*
563 *parvum*. J. Plankton Res. 31, 301-309.
564 Oksanen, J., Blanchet, F.G., Kindt, R., Legendre, P., Minchin, P.R., O'Hara, R.B.,
565 Simpson, G.L., Solymos, P., Stevens, M.H.H. and Wagner, H., 2014. Vegan:
566 Community Ecology Package. R Package Version 2.2-0.
567 Pérez-Ruzafa, A., Campillo, S., Fernández-Palacios, J.M., García-Lacunza, A., García-
568 Oliva, M., Ibañez, H., Navarro-Martínez, P.C., Pérez-Marcos, M., Pérez-Ruzafa,
569 I.M., Quispe-Becerra, J.I., Sala-Mirete, A., Sánchez, O., Marcos, C., 2019. Long-
570 term dynamic in nutrients, chlorophyll *a*, and water quality parameters in a coastal
571 lagoon during a process of eutrophication for decades, a sudden break and a
572 relatively rapid recovery. Front. Mar. Sci. 11,
573 https://doi.org/10.3389/fmars.2019.00026
574 Pérez-Ruzafa, A., Marcos, C., Gilabert, J., 2005. The ecology of the Mar Menor coastal
575 lagoon: a fast changing ecosystem under human pressure. In: Gönenç, I.E., Wolflin,
576 J.P. (Eds.). Coastal Lagoons: Ecosystem Processes and Modeling for Sustainable Use
577 and Development. CRC Press, Boca Ratón, Florida: 392-422.
578 Phlips, E.J., Badylack, S., Lynch, T.C., 1999. Blooms of the picoplanktonic
579 cyanobacterium Synechococcus in Florida Bay, a subreopical inner-shelf lagoon.

580 Limnol. Oceanogr. 44, 1166-1175.
581 Ramírez, T., Cortés, D., Mercado, J.M., Vargas-Yáñez, M., Sebastián, M., Liger, E.,
582 2005. Seasonal dynamics of inorganic nutrients and phytoplankton biomass in the
583 NW Alboran Sea. Estuar. Coast. Shelf. Sci. 65, 654–70.
584 R Core Team (2013). R: A language and environment for statistical computing. R
585 Foundation for Statistical Computing, Vienna, Austria. URL http://www.R-
586 project.org/
587 Romo S, García-Murcia A, Villena MJ, Sánchez V, Ballester A. (2008) Albufera de
588 Valencia and implications for its ecology, management and recovery. Limnetica 27:
589 11-28
590 Roy, S., 1989. HPLC-measured chlorophyll-type pigments during a phytoplankton
591 spring bloom in Bedford Basin (Canada). Mar. Ecol. Prog. Ser. 55 : 279-290.
592 Ruíz, J,M, Albentosa, M., Campillo, J.A., León, V.M., et al., 2016. Programa de
593 seguimiento de la eutrofización en la laguna costera del Mar Menor. Report of the
594 Project MEMM. Instituto Español de Ocenografía. 33 pp.
595 Ruíz, J.M., Abentosa, M., Aldeguer, B., Álvarez-Rogel, J., Antón, J., Belando, M.D.,
596 Bernardeu, J., Campillo, J.A., Domínguez, J.F., Ferrera, I., Fraile-Nuez, E., García,
597 A., Gómez-Ballesteros, M., Gómez, F., González-Barberá, G., Gómez-Jakobsen, F.,
598 León, V.M., López-Pascual, C., Marín-Guirao, L., Martínez-Gómez, C., Mercado,
599 J.M., Nebot, E., Ramos, A., Rubio, E., Santos, F., Vázquez-Luis, M., Yebra, L.,
600 2020. Informe de evaluación y estado actual del Mar Menor en relación al proceso de
601 eutrofización y sus causas. Informe de asesoramiento técnico del Instituto Español de
602 Oceanografía (IEO). 165 pp.
603 Simis, S.G., Peters, S.W., Gons, H.J., 2005. Remote sensing of the cyanobacterial
604 pigment phycocyanin in turbid inland water. Limnol. Oceanogr. 50, 237-245.
605 Soja-Wozniak M, Darecki M, Wojtasiewicz B, Bradtke K (2018) Laboratory
606 measuremens of remote sensing reflectance of selected phytoplankon species from
607 the Baltic Sea. Oceanologia 60:86-96
608 Soria, J., Caniego, G., Hernández-Sáez, N., Erena, M., 2019. Phytoplankton distribution
609 in Mar Menor Coastal Lagoon (SE Spain) during 2017. Preprints 2019120277
610 Sunda, W.G., Graneli, E., Gobler, C.J., 2006. Positive feedback and the development
611 and persistence of disruptive algal blooms. J. Phycol. 42, 963-974.

612 Sunda, W.G., Shertzer, K.W., 2012. Modeling ecosystem disruptive algal blooms:
613 Positive feedback mechanisms. Mar. Ecol. Prog. Ser. 447, 31-47.
614 Terrados, J., Ros, J., 1991. Production dynamics in a macrophyte-dominated ecosystem
615 the Mar Menor coastal lagoon (SE Spair). Oecologia Aquat. 10, 255–270.
616 Tomas, C.R., 1997. Identifying Marine Phytoplankton. Academic Press Limited,
617 London. 858 pp.
618 Trice, T.M., Glibert, P.M., Lea, C., Van Heukelem, L., 2004. HPLC pigment records
619 provide evidence of past blooms of *Aureococcus anophagefferens* in the Coastal
620 Bays of Maryland and Virginia, USA. Harmful Algae. 3, 295–304.
621 Warmer, R.A., Fan, C., 2013. Optical Spectra of Phytoplankton Cultures for Remote
622 Sensing Applications: Focus on Harmful Algal Blooms. Int. J. Environ. Devel. 4, 94-
623 98.
624 Wojtasiewicz, B., Stoń-Egiert, J., 2016. Bio-optical characterization of selected
625 cyanobacteria strains present in marine and freshwater ecosystems. J. Appl. Phycol.
626 28, 2299-2314.
627 Zhang, X., Kan, J., Wang, J., Gu, H., Ju, J., Zhao, Y., Sun, J., 2015. Fist record of a
628 large-scale bloom causing causes species *Nannochloropsis granulata* ole1430-1441.
629
630

Table 1. Environmental variables determined during the monthly samplings. The means are averaged values for the three stations and samples collected at each sampling. Units: temperature (T), ºC; nutrient concentrations, µM; chorophyll *a* concentration (Chl *a*), µg L^{-1}.

	2016*			**2017**			**2018**			**2019***		
	min	max	mean	min	max	mean	min	max	mean	min	max	mean
T (ºC)	22.1	27.5	25.2	10.5	30.4	21.9	12.1	29.4	19.9	11.7	29.0	18.5
Salinity	43.6	46.5	45.3	39.3	44.7	42.7	43.3	46.8	44.8	42.9	46.4	44.5
Nitrate	0.35	1.43	0.79	0.06	9.2	3.7	0.15	3.7	1.3	0.04	1.94	0.58
Nitrite	0.02	0.07	0.04	0.07	0.39	0.19	0.02	2.9	0.44	0.13	0.19	0.15
Phosphate	0.02	0.22	0.09	0.04	0.11	0.07	0.03	0.35	0.23	0.11	0.21	0.15
Silicate	23.1	47.0	37.0	12.0	51.1	30.4	0.13	27.2	14.9	0.85	45.3	13.2
Chl *a*	5.	12.2	9.3	1.5	10.6	3.9	0.6	6.2	2.4	0.4	24.2	4.2

*Note that the sampling period was May-December in 2006 and January-October in 2019; therefore, the data do not cover the whole annual cycle

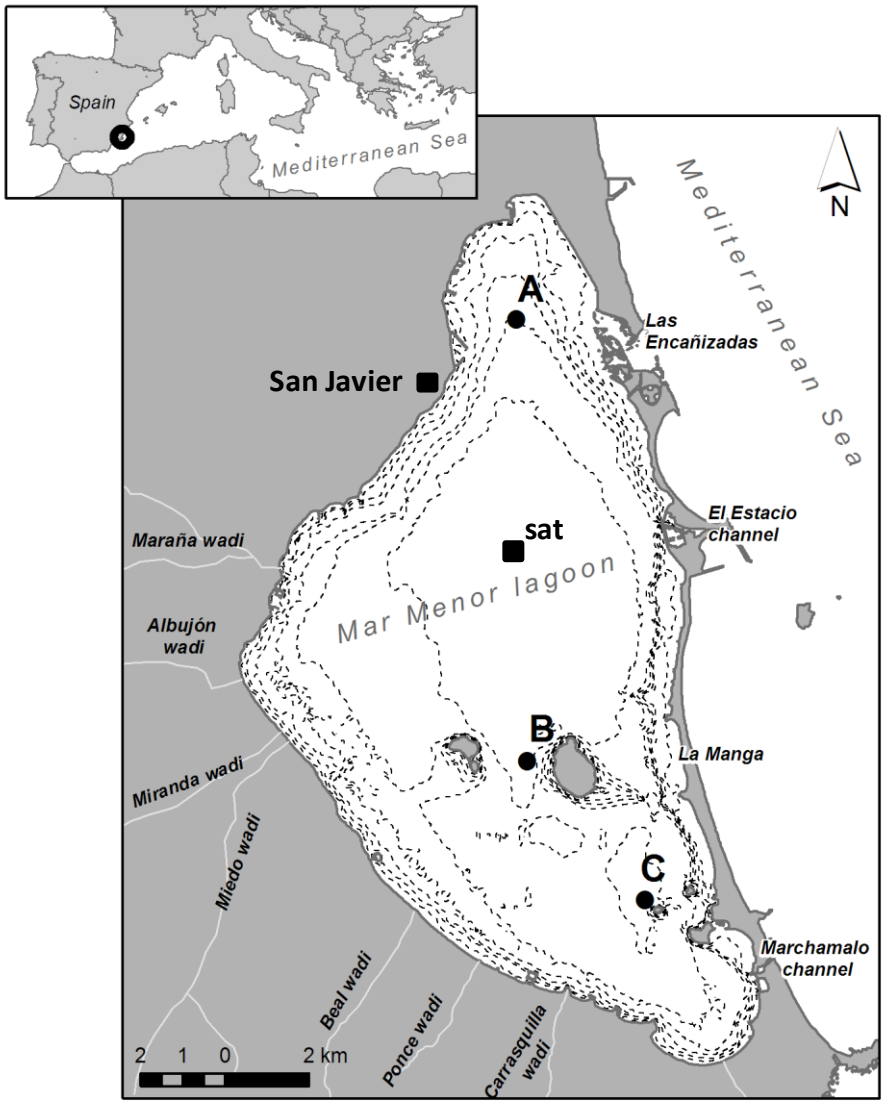

Fig. 1. Map of the Mar Menor showing the location of the sampling stations (A, B and C), the position of the pixel used to build time series of satellite data (sat) and the location of the meteorological station (San Javier).

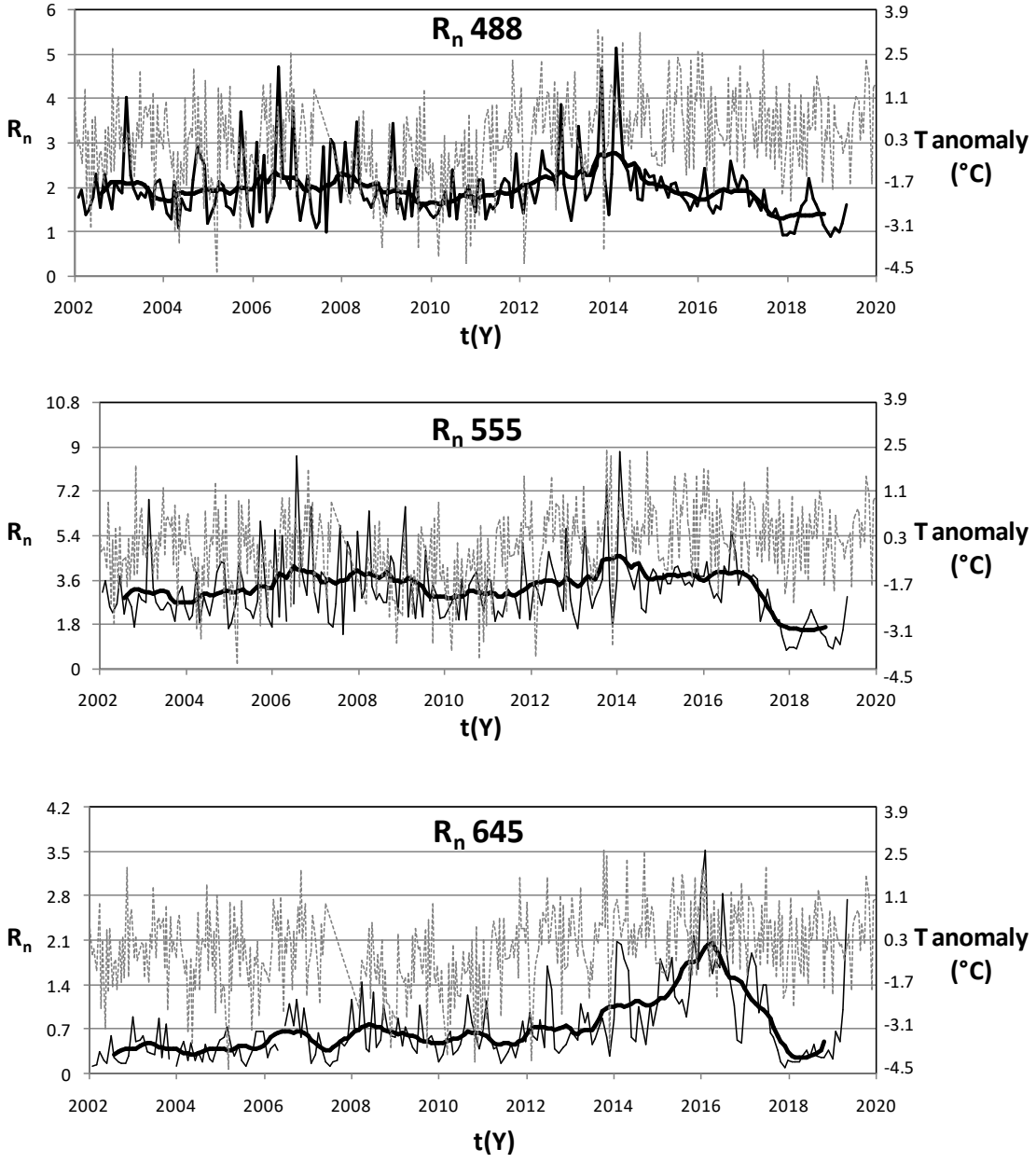

Fig. 2. Mean monthly values of three selected satellite reflectance bands (R_n488, R_n555, R_n645). The thick black line indicates the trend series calculated after seasonal decomposition of the raw series (thin black line). The time series of atmospheric temperature anomalies is also shown (grey dashed line).

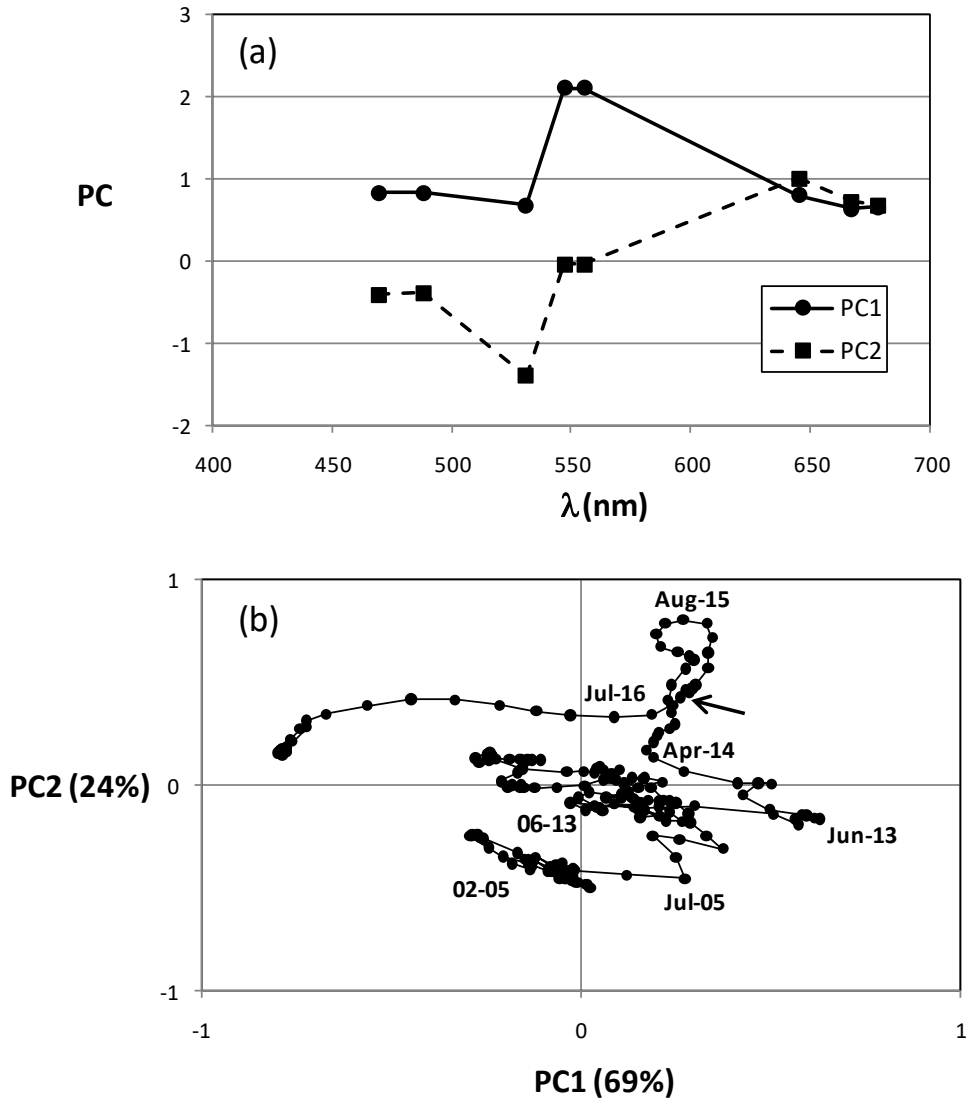

Fig. 3. Results of the principal component analysis performed with the trend series of the different satellite reflectance bands. (a) Two first variance component scores (PC) of each reflectance band; (b) Scores of each monthly period for the two first variance components.

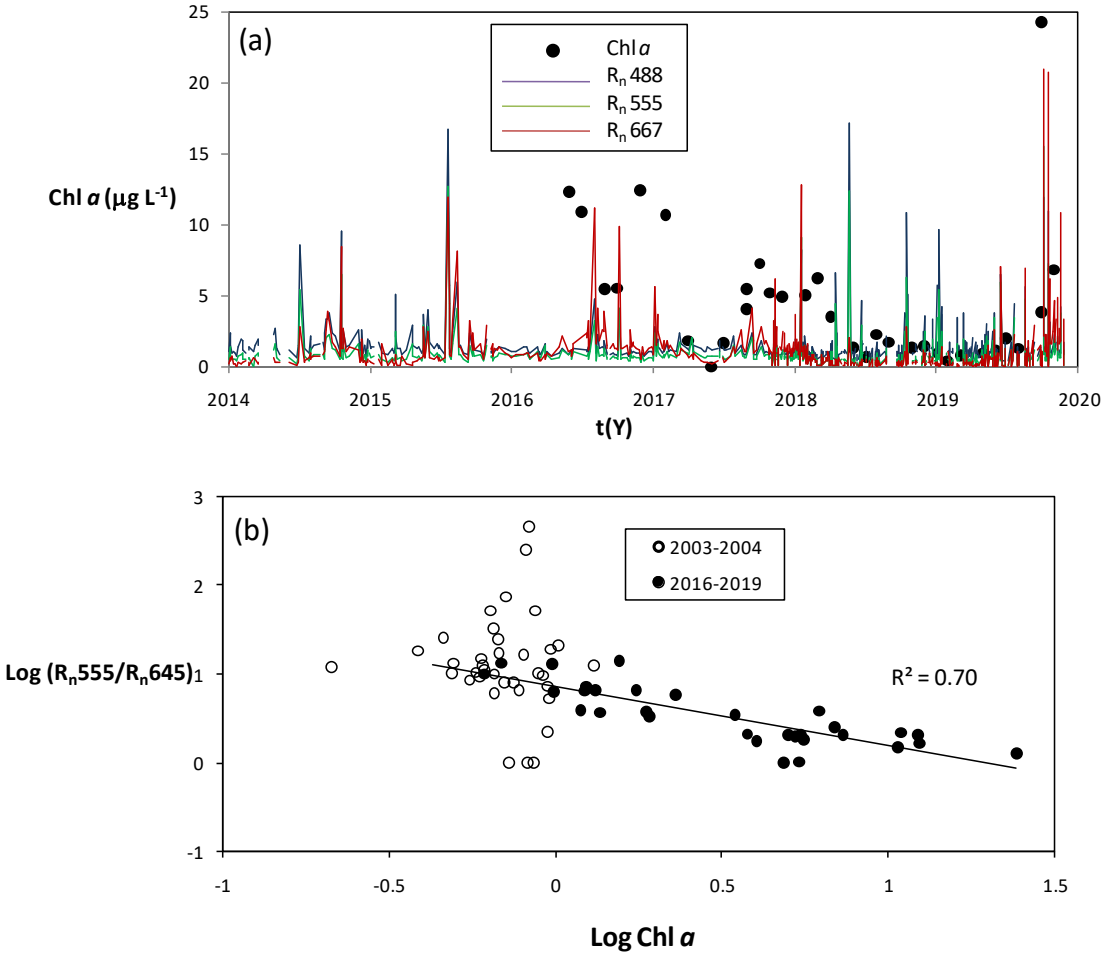

Fig. 4. Time changes in the chlorophyll *a* concentration averaged from the three stations sampled monthly and their relation with satellite reflectance. (a) Monthly chlorophyll *a* concentration. Time series of daily R_n at some selected bands obtained during the period 2014-2019 are shown; (b) correlation between chlorophyll *a* and R_n550/R_n645 ratio for the period 2016-2019, calculated with the R_n values roughly matching with the sampling date (±48 h).

675

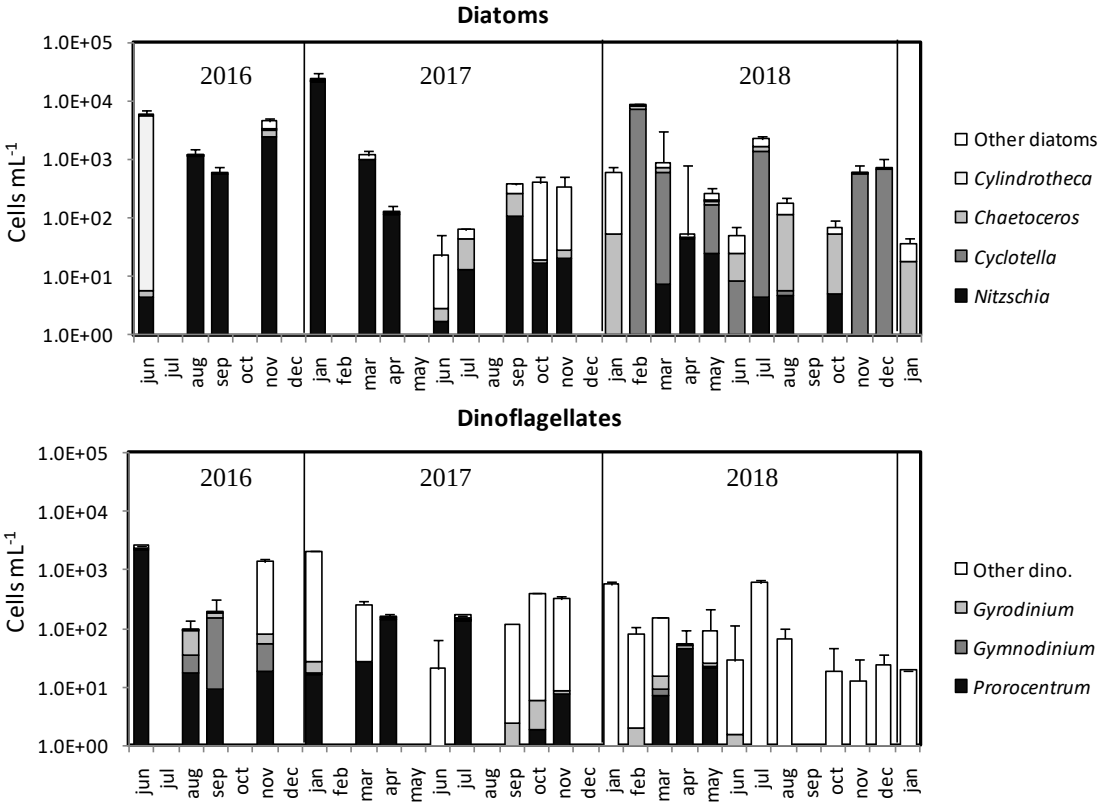

676

677 **Fig 5.** Cell abundance monthly means of the main groups of diatoms and dinoflagellates
678 identified in the analyzed samples. Note that the abundances are shown in logarithm
679 scale. Vertical lines on the bars indicate the standard deviation.

680

681

682

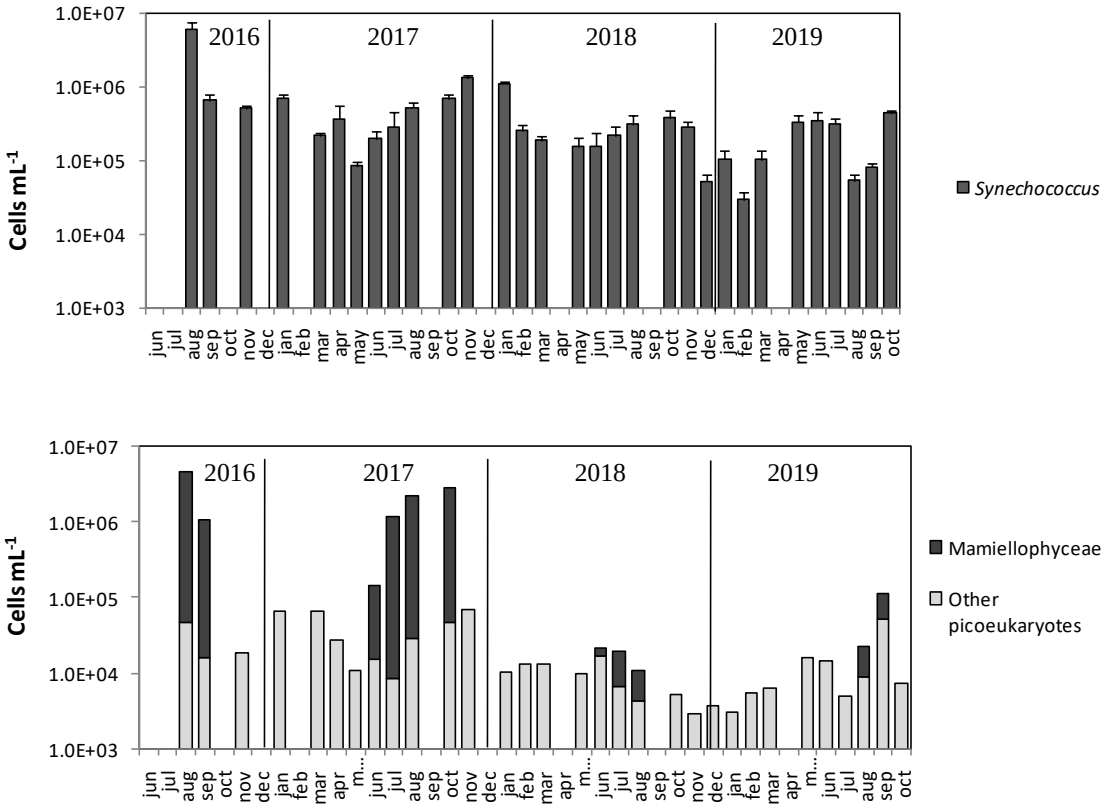

Fig. 6. Cell abundance monthly means of *Synechococcus* and picoeukaryotes. Note that the abundances are shown in logarithm scale. Vertical lines on the bars indicate the standard deviation of three sampling stations.

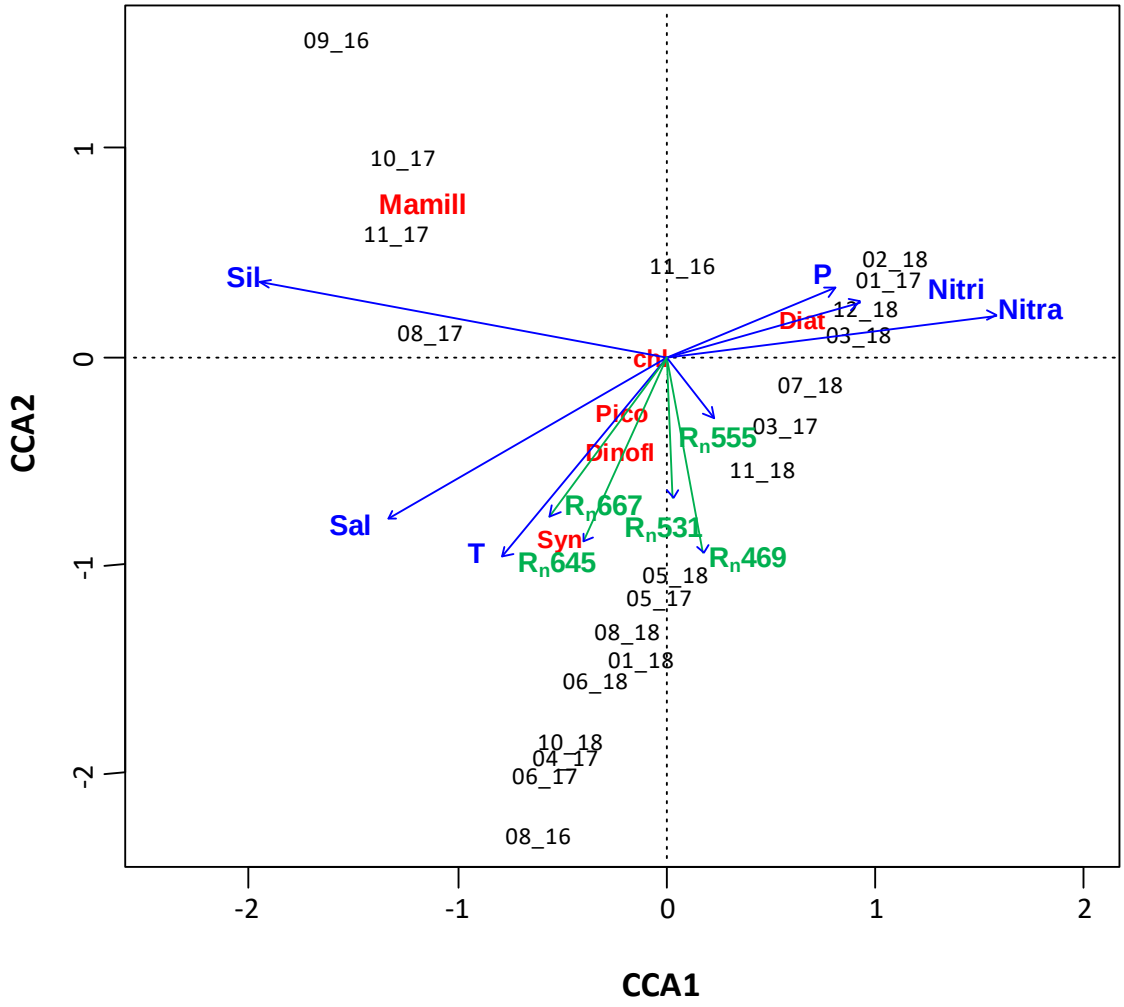

692

693 **Fig 7.** Biplot of the scores obtained from the canonical correspondence analysis. T:
694 temperature; Sal: salinity; Sil: silicate; Nitra: nitrate concentration; Nitri: nitrite
695 concentration; P: phosphate; Chl: chlorophyll *a*; Diat: diatoms; Dinofl: dinoflagellates;
696 Syn: *Synechococcus*; Mamill: Mamiellophyceae; Pico: other picoeukaryotes.

697

698

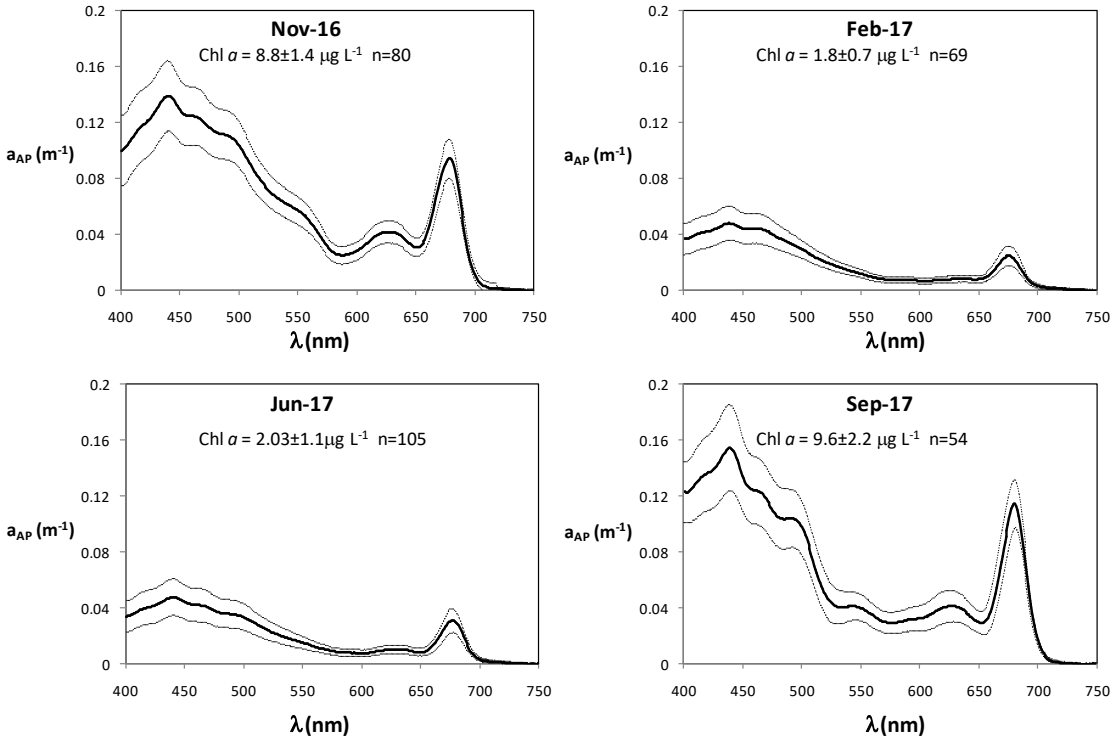

Fig 8. Phytoplankton absorption spectra averaged (continuous line) ± 1SD (dotted lines). Concentration of chlorophyll *a* averaged and amount of samples analyzed are indicated.

706

707

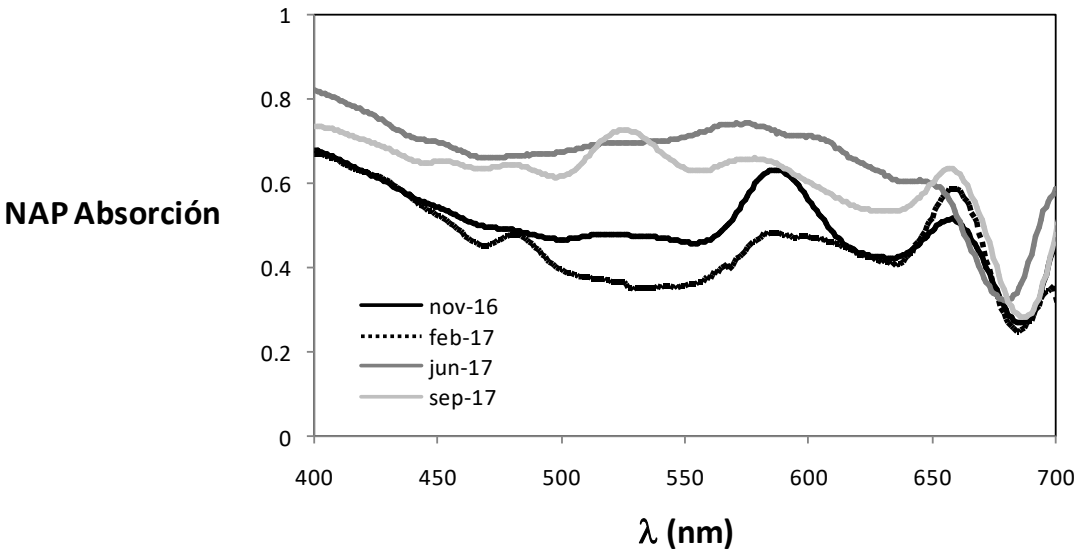

708

709 **Supplementary Fig. 1.**Spectral contribution mean of the non-algal particles to the
710 particle matter absorption for the four samplings performed in 2016-2017.

711